The Direct Smooth Muscle Myosin Inhibitor, CK-2018571, Represents a Novel Therapeutic Mechanism for Bronchodilation

Zhiheng Jia, Guillermo Godinez, Nickie Durham, Xi Wang, Chihyuan Chuang, Pu-Ping Lu, Wenyue Wang, Bing Yao, Jeffrey Warrington, Sheila Clancy, James J Hartman, David J Morgans Jr, Bradley P Morgan, Xiangping Qian, Fady I Malik, Malar Pannirselvam

Cytokinetics, Inc., South San Francisco, CA, USA.

Introduction

Smooth muscle myosin is a mechanochemical enzyme that hydrolyzes ATP to generate mechanical force; ultimately all signaling pathways that modulate smooth muscle tone converge onto the regulation of this motor protein. Using high throughput screening, we identified and subsequently optimized a class of selective inhibitors of smooth muscle myosin. Previously we showed that CK-2018509, a novel, potent, and selective inhibitor of the enzymatic activity of smooth muscle myosin, decreased the mean arterial pressure in two animal models of hypertension [1]. Another novel smooth muscle myosin inhibitor, CK-2019165, an active pro-drug of CK-2018571, was previously shown to decrease right ventricular systolic pressure in two rat models of pulmonary arterial hypertension [2]. Given its central role in generating smooth muscle contractility in the settings of chronic obstructive pulmonary disease (COPD) and asthma, direct inhibition of smooth muscle myosin could provide a novel and effective means to reduce bronchoconstriction in asthma and COPD. The objective of the present study was to evaluate the pharmacology of CK-2018571 and CK-2019165 in rat models of bronchoconstriction.

Methods

Biochemical Assays: Assays were performed in low salt PM12 buffer (12 mM K-Pipes, 2 mM $MgCl_2$, pH 6.8) in the presence of actin and 250 µM ATP (>5-10-fold above the $K_{M,ATP}$). Hydrolysis rates were normalized using reactions containing an equivalent amount of DMSO.

Myosin binding was measured by depletion of soluble myosin from binding reactions using smooth muscle myosin S1 fragment (chicken, recombinant) and 5 µM bovine cardiac actin. ATP and ADP were included at 1 mM where indicated. Reactions were allowed to equilibrate for 15 minutes prior to centrifugation (540k x g, 30 minutes), however ATP was added just prior to centrifugation to minimize hydrolysis. Supernatants were analyzed by SDS-PAGE followed by staining with Coomassie brilliant blue.

Skinned Ring Assay: Endothelium-denuded rat tail artery segments were cut into 3-mm helical rings, mounted on an isometric force transducer with a resting tension of 0.5 g and incubated for 30 minutes at room temperature in normal H-T buffer. Tissues were incubated with skinning solution containing 1% Triton X-100 for 1 hour at room temperature. CK-2018571 was added to the tissue for 15 minutes, followed by addition of solutions with increasing calcium. Force was recorded at each calcium concentration. Data were presented as a percent change from the baseline values.

Tracheal Ring Assay: The trachea was removed and placed in Krebs-Henseleit buffer aerated with 95% O_2 and 5% CO_2. The trachea was cut into 2 mm rings, mounted on a tissue bath apparatus, and maintained at a baseline tension of 2 g. CK-2018571-induced relaxation was recorded in preparations pre-contracted with a sub-maximal concentration of methacholine (3 µM).

Thiophosphorylation Assay: Triton-permeabilized preparations were incubated in rigor solution containing ATPγS (1 mM) for 10 minutes. CK-2018571 was added 15 minutes before addition of the ATP. ATP induced contraction was measured for 60 minutes and the relaxation was expressed as the percentage of the maximum force.

***In vivo* Assay:**

Anesthetized Rodent Model of Airway Resistance & Compliance

Male Sprague-Dawley rats were anesthetized with Ketamine/Xylazine/Acepromazine (80/10/1 mg/kg) cocktail and tracheotomized with a 14 g tracheal cannula. Rats were paralyzed with Pancuronium Bromide at 2 mg/kg, *i.p.* to prevent spontaneous breathing. Immediately rats were placed on a Resistance & Compliance Plethysmograph (Buxco Research Systems). Once rats were stabilized and a baseline was collected, CK-2019165 was intra-tracheally nebulized via an Aeroneb Lab micropump nebulizer. Five minutes later, dose dependent bronchoconstriction to methacholine was measured.

Conscious Rodent Model of Unrestrained Whole Body Plethysmography

Male Spraque-Dawley rats were dosed with CK-2019165 via conscious spontaneous inhalation of aerosolized solution in an in-house custom built 12-slot closed pie chamber using a PARI LC Plus Jet Nebulizer (22F80, PARI Respiratory Equipment), pressurized to 22 psi with a carrier gas mixture of 21% O_2, 5% CO_2, 74% N_2 with a flow rate of 12 L/min. After dosing, rats were placed in an Unrestrained Whole Body Plethysmograph (Buxco Research Systems), and animals were allowed to acclimate. A baseline measurement was collected and rats were subsequently challenged with nebulized methacholine (100 µL/rat of 20 mg/mL).

Results

Figure 1: CK-2018571 selectively inhibits the ATPase activity of smooth muscle myosin

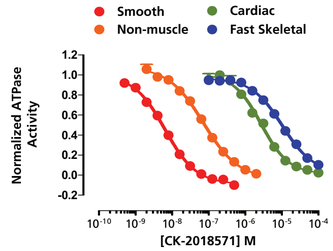

Myosin Isoform	IC_{50} ± SD, nM
Smooth	9.0 ± 4.8
Non-muscle IIB	76 ± 4.9
Cardiac	2600 ± 240
Fast skeletal	11,300 ± 840

Inhibition of the Mg^{2+}-ATPase activity of smooth muscle (human recombinant), non-muscle IIB (human recombinant), cardiac (bovine native), and fast skeletal (rabbit native) S1 fragments at varying concentrations of CK-2018571. ATPase activity was measured in the presence of actin and 250 µM ATP (~5-10-fold above the $K_{M,ATP}$). ATPase rates were normalized to reactions containing an equivalent amount of DMSO. Representative curves from duplicate reactions are shown in the graph. Pooled results from three experiments are shown in the table.

Figure 2: CK-2018571 does not promote strong actomyosin binding

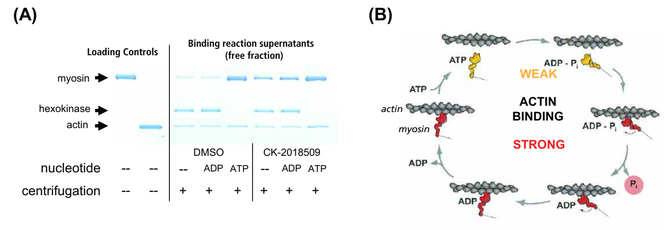

Actomyosin binding of soluble smooth muscle myosin (recombinant S1 fragment, chicken) in the presence of actin and various nucleotides **(A)**. Total amounts of myosin (3 µM) and actin (5 µM) are indicated by the loading controls (left), while unbound myosin is shown in the supernatant fractions of the binding reaction (right). **(B)** Smooth muscle myosin chemo-mechanical cycle, indicating weak and strong actin binding states.

Figure 3: CK-2018571 inhibits calcium-induced contraction of skinned caudal artery smooth muscle preparation

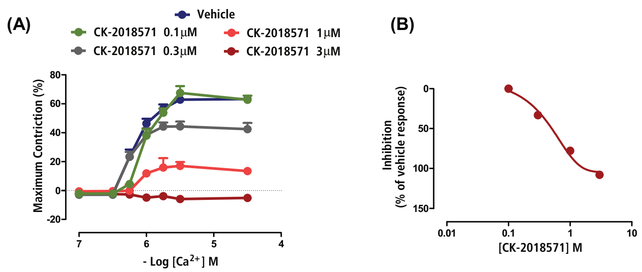

(A) Mean pCa-response curves in the presence (0.1, 0.3, 1 & 3 µM) or absence of CK-2018571 in skinned caudal artery rings from Sprague Dawley rats (n=2-4). Symbols are mean ± standard error values. **(B)** Concentration-response curve for CK-2018571 constructed from the maximal inhibition of calcium-induced contraction from figure **(A)**. CK-2018571 inhibited the calcium induced forced development of the skinned caudal ring in a concentration dependent manner with an EC_{50} of 0.9 µM and E_{max} of 105%. Symbols are mean values.

Figure 4: CK-2018571 causes concentration dependent relaxation of isolated tracheal rings

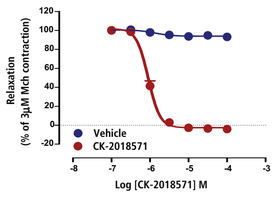

Concentration-response curve to CK-2018571 in isolated tracheal rings (n=11-12) pre-constricted with 3 µM methacholine from Sprague Dawley rats. CK-2018571 relaxed the isolated tracheal rings in a concentration-dependent manner with an EC_{50} of 0.9 µM and E_{max} of 105%. Symbols are mean ± standart error values.

Figure 5: CK-2018571 relaxes the ATP-induced contraction in ATPγS treated skinned caudal artery

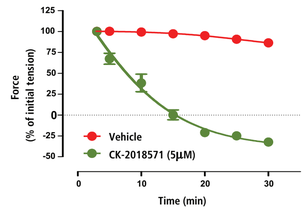

Force development to ATP in the presence or absence of CK-2018571 (5 µM) in isolated skinned and thiophosphorylated aortic rings (n=8-12) from Sprague Dawley rats. Symbols are mean ± standard error values.

Figure 6: CK-2019165 inhibited the methacholine-induced bronchoconstriction in anesthetized, paralyzed and mechanically ventilated resistance and compliance rat model

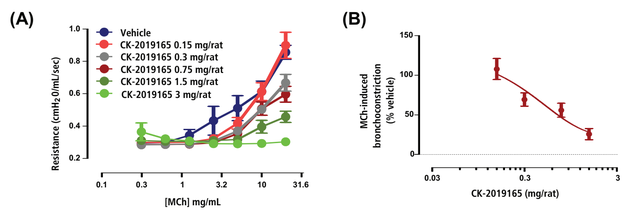

(A) Effect of CK-2019165 on methacholine-induced bronchoconstriction in anesthetized, paralyzed and mechanically ventilated rats (n=3-7 rats). Symbols are mean ± standard error values. **(B)** Dose-response curve for CK-2019165 showing dose-dependent inhibition of methacholine-induced bronchoconstriction with an EC_{50} of 0.7 mg/rat and E_{max} of 74%. Symbols are mean ± standard error values.

Figure 7: CK-2019165 inhibited the methacholine-induced bronchoconstriction in unrestrained whole body plethysmography rat model

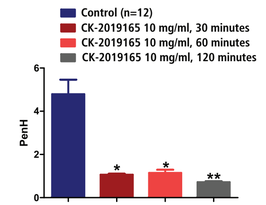

* P< 0.05 & **P< 0.01 compared to control by one-way ANOVA followed by Bonferroni *post hoc* test

Effect of CK-2019165 on methacholine-induced bronchoconstriction in unrestrained whole body plethysmography in rats (n=3-12 rats). Each bar represents mean PenH ± standard error values.

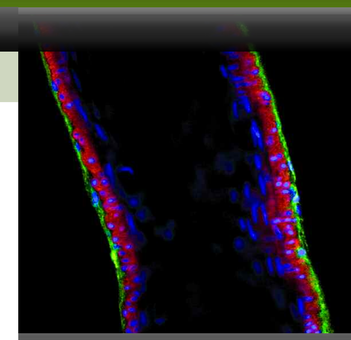

Conclusions

1. CK-2018571 selectively inhibits the ATPase activity of smooth muscle myosin over other myosin II isoforms (non-muscle myosin, cardiac and fast skeletal muscle myosin).
2. CK-2018571 inhibits smooth muscle myosin in a weak actin-binding state.
3. CK-2018571 inhibits calcium-induced force development in skinned caudal artery and relaxes skinned rings activated by thiophosphorylation, consistent with relaxation occurring as a consequence of direct inhibition of smooth muscle myosin.
4. CK-2018571 relaxes methacholine pre-constricted tracheal rings in a concentration dependent manner suggesting its potential use as a bronchodilator.
5. CK-2019165 inhibited the methacholine-induced bronchoconstriction in two rat models of bronchoconstriction, i.e. resistance and compliance model and unrestrained whole body plethysmography.

These data together suggest that direct inhibition of smooth muscle myosin could be a novel therapeutic approach for the treatment of chronic obstructive pulmonary disease and asthma.

References

1. Qian X, Wang X, Hartman JJ, Jia Z, Yao B, Chuang C, Lu P, Pannirselvam M, Morgans DJ, Morgan BP, Malik FI. A direct inhibitor of smooth muscle myosin as a novel therapeutic approach for the treatment of systemic hypertension. The Journal of Clinical Hypertension, 2009; **11(4)**: A37
2. Pannirselvam M, Durham N, Jia Z, Clancy S, Chuang C, Lu P, Wang W, Yao B, Warrington J, Hartman JJ, Morgans Jr DJ, Morgan BP, Qian X, Malik FI,. A direct inhibitor of smooth muscle myosin as a novel therapeutic approach for the treatment of pulmonary artery hypertension. Circulation. 2009;**120**:S805

CYTOKINETICS